

# The design of “multiple energies from one source” in D-T neutron tube

Hui-Ping Guo<sup>1</sup> · Kuo Zhao<sup>1</sup> · Ning Lü<sup>1</sup> · Zhi-Hao Wei<sup>1</sup> · Wen-Hui Lü<sup>1</sup>

Received: 24 March 2015 / Revised: 24 September 2015 / Accepted: 3 November 2015 / Published online: 24 August 2016  
© Shanghai Institute of Applied Physics, Chinese Academy of Sciences, Chinese Nuclear Society, Science Press China and Springer Science+Business Media Singapore 2016

**Abstract** To obtain multiple monoenergetic neutron sources and realize the on-site calibration of radiation monitoring equipment for nuclear-involved places, the structural characteristics and neutron source features of D-T neutron tube were analyzed; Monte Carlo method was adopted to simulate the effect of interaction between typical materials and different energy neutrons; multilayered shielding materials were combined and optimized to acquire the optimal scheme to shield the neutron sources from the neutron tube. On the base, a tapered alignment filtration construction was designed and Monte Carlo method was employed to simulate the effect of alignment construction. The result showed that the tapered alignment filtration construction can create monoenergetic neutrons including 14.1 MeV, 0.18 MeV and thermal neutrons and demonstrated good monochrome performance which provides multiple monoenergetic sources for the on-site calibration.

**Keywords** Neutron tube · Monte Carlo method · Shielding · Alignment system

## 1 Introduction

To obtain the monoenergetic neutron sources, standard source items [1, 2] should be available for the on-site calibration of neutron radiation monitoring instrument and the neutron tubes, which have advantages of low cost, easy protection and maintenance, lightweight and simple

operation (regarded as one of source items with wide popularity) [3–5]. However, disadvantages of launching at  $4\pi$  angle of neutron sources and the single energy point can restrict the application of neutron tubes to on-site calibration. To solve this problem, Monte Carlo method was adopted in this paper to analyze the effects of interactions between typical materials and different energy neutrons. With the obtained optimal shielding structure of neutron sources from the neutron tubes, a tapered alignment filtration system was designed to restrict the launching angle. Then, we obtained the monoenergetic neutrons with different energies to realize “multiple energies from one source” in the neutron tubes.

## 2 Theoretical analysis

D-T neutron tubes are mainly characterized by no radiation without powers, outgoing neutron being the monoenergetic neutrons approximately [6], average energy of 14.1 MeV and isotropy of neutron outgoing. To obtain the monoenergetic neutrons, it is necessary to design a layer of shielding filtration structure to filter the neutrons with approximate isotropy and transfer them into monoenergetic neutrons. First of all, shielding structure studies should be carried out. Heavy materials are used to moderate fast neutrons for they have larger inelastic scattering section [7, 8]. Hydrogenous materials with larger elastic scattering section can carry out further slowing down to decrease the neutron energy to the thermal neutron zone. And the thermal neutrons can be absorbed through nuclear reaction ( $n, x$ ) which retains the neutrons inside the shield, so as to achieve the goal of shielding. Normally, the absorption section of boron is relatively large [9], but  $\alpha$  charged particles and secondary  $\gamma$  ray will be generated at the same time

✉ Kuo Zhao  
zhao13772073797@163.com

<sup>1</sup> Xi'an Research Institute of Hi-Tech, Xi'an 710025, China

if boron is used as shielding materials. The range of  $\alpha$  ray is short and easily shielded. Finally, the heavy metal materials, such as lead, are applicable to realize the target of shielding  $\gamma$  ray [10–12]. Therefore, it is proposed to set four layers of shielding material to shield the fast neutrons which are produced by neutron tubes, as shown in Fig. 1.

### 3 Design and verification of optimal shielding structure

#### 3.1 Structure design

Since the average energy of outgoing neutron is 14.1 MeV, metal materials like copper (Cu), ferrum (Fe) and tungsten (W) can be chosen to slow down and transfer 14.1 MeV into intermediate and low-energy neutrons [13–15]. At this moment, hydrogenous materials with larger elastic scattering cross section such as polyethylene and water can be selected to further slow down the neutrons [16]. And the third layer is neutron absorption material. Boron has relatively large absorption cross sections, so  $B_4C$  can be selected to absorb the thermal neutrons [17, 18], but in this process, a large amount of secondary  $\gamma$  rays will occur [19, 20]. To reduce as many as  $\gamma$  rays, lead is proposed to absorb  $\gamma$  photons to obtain the optimal structure. To create enough space inside the shield, it is planned to adopt cuboid structure for the shield and there is a cuboid cavity with a dimension of  $5\text{ cm} \times 5\text{ cm} \times 240\text{ cm}$  in the shield (shown in Fig. 2 without the red tapered alignment hole) considering the structure size of the neutron tubes (investigated in this paper).

#### 3.2 Simulation verification

To acquire the thickness of all layers of shielding materials, MCNP program will be employed to simulate layer by layer. The materials with different thicknesses and types are

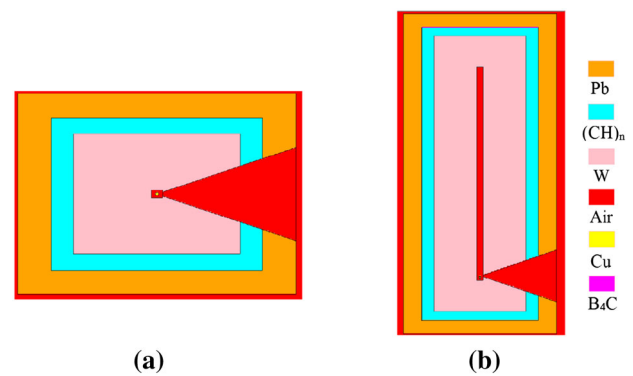


**Fig. 2** Scheme of collimating structure: **a** horizontal and **b** vertical section

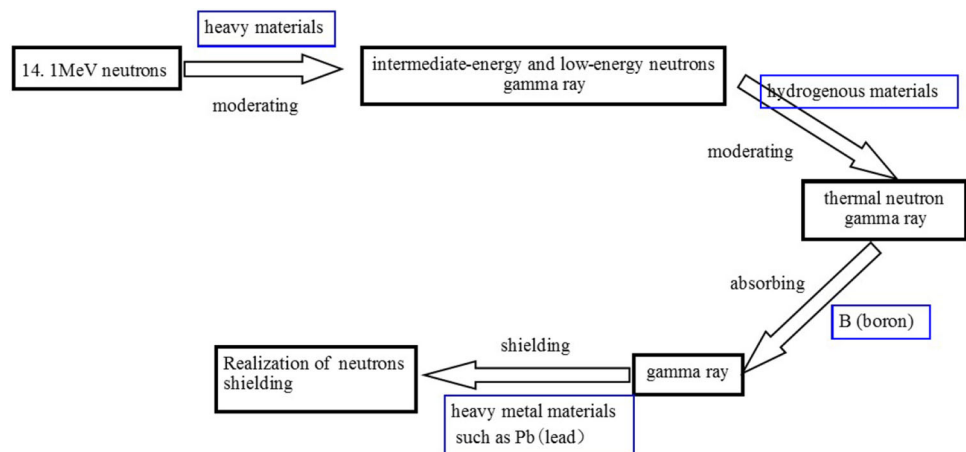
used for combined comparison. The materials mentioned by former section at first three layers are typed into MCNP software simultaneously. The types of materials at the first and second layer and the thickness of materials at the third layer are changed. The corresponding changing curves of neutron fluence that varies with energy transformation are displayed in Fig. 3. It can be seen that the neutron fluence decreases to below 0.025 %. Accordingly, six combining schemes of the first three layers of materials can be obtained.

In order to sharply alleviate the influence of  $\gamma$  ray on the neutron radiation field, lead is proposed to be used as the shielding materials for the third layer. Under the combining schemes of the first three layers, the variation of  $\gamma$  relative fluence with the thickness of Pb is displayed in Fig. 4. According to Fig. 4, it is suitable to determine the thickness of lead shielding layer as 10 cm.

### 4 Design and verification of alignment structure

The D-T neutron tube excites neutrons with average energy of 14.1 MeV at  $4\pi$  angle direction. To realize the result of “multiple energies from one source” of neutron

**Fig. 1** Principle of neutrons slowing down



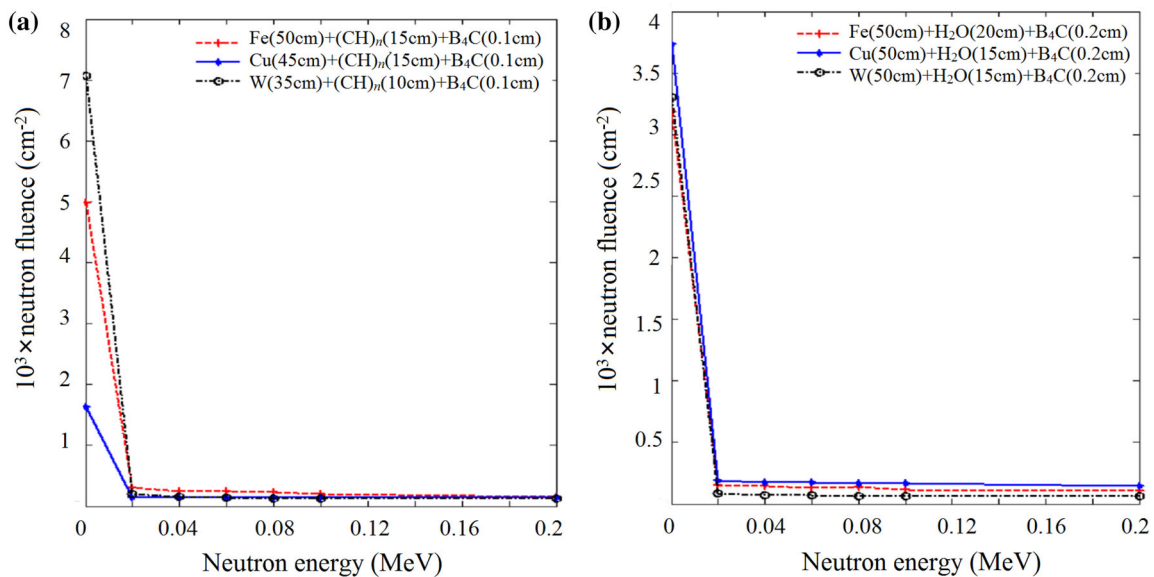


**Fig. 3** Neutron fluence versus energy

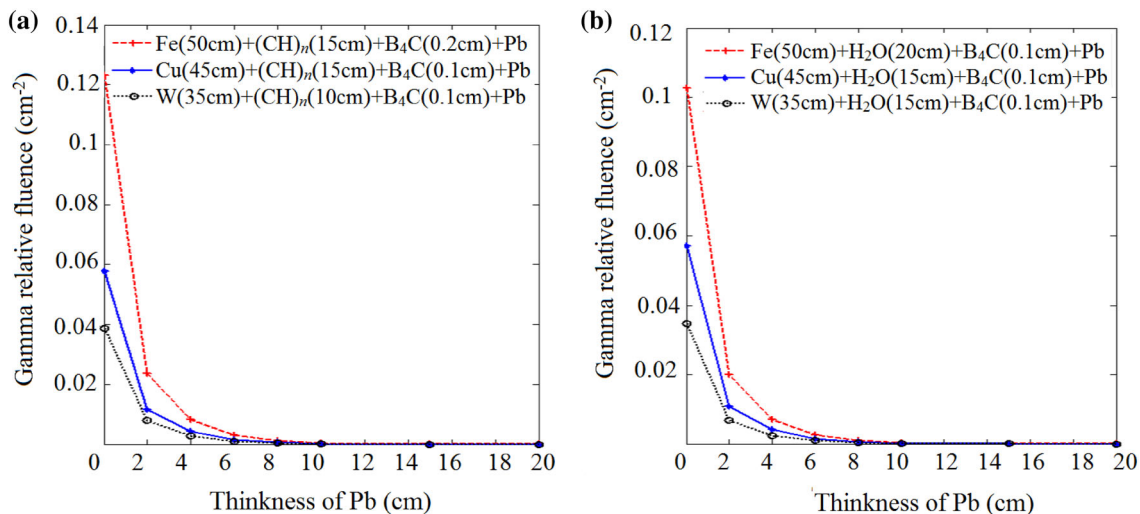


**Fig. 4** Gamma relative fluence versus thickness of Pb

source, it is necessary to design a neutron alignment filtration structure. General neutron alignment structures include cylindrical outlet structure, multitube outlet structure and tapered outlet structure.

The neutron shielding filtration system in this paper will be applied to calibration research, so outgoing neutron should cover the whole detector zone. Considering that cylindrical outlet structure and multitube outlet structure have relatively small coverage, thus this paper adopts tapered outlet structure as the neutron alignment structure. In the meanwhile, due to neutrons with different energies having different cross sections on the materials, after the neutrons (from the neutron tubes) are slowed down and absorbed by filtration mediums, neutron energy can gather at a certain segment, thus forming quasi-monoenergetic neutrons.

#### 4.1 14.1 MeV monoenergetic neutron

##### 4.1.1 Design

The neutron source of D-T neutron tube can outgo the neutrons with average energy of 14.1 MeV and the neutron energy range is relatively narrow, so it can be approximately viewed as monoenergetic neutron source. To obtain 14.1 MeV quasi-monoenergetic neutrons, a tapered alignment hole should be designed on the shielding structure and 14.1 MeV monoenergetic neutrons can be directly obtained without any shielding. In consideration of the size of shielding structure, the scheme of W (35 cm) + (CH)<sub>n</sub> (10 cm) + B<sub>4</sub>C (0.1 cm) + Pb (15 cm) is taken as the example to design the alignment structure. The tapered alignment hole has an axial symmetry

structure which guarantees that the tapered alignment projection can completely cover the monitor at the location (1 m from the source center), with a taper angle of  $25^\circ$ , and the alignment structure is displayed in Fig. 2.

But due to scattering effects of various materials, a lot of scattering neutrons will generate. The primary scattering neutrons include two parts. The first part includes the scattering neutrons created by interaction between the innermost shielding materials and 14.1 MeV neutrons; the other part contains the scattering neutrons produced by interaction of alignment hole inner surface and neutrons as well as the neutrons leaked from the alignment hole inner surface in the transportation process of shielding layer.

In addition, through simulation of variation of scattering neutrons with material thickness, W shows good scattering effect on 14.1 MeV neutrons. To reduce as many as impacts of scattering neutrons, a kind of materials with weak scattering effect on 14.1 MeV neutrons is added to the innermost shielding layer. Based on the simulation result, at the innermost shielding layer, a layer of boracic polyethylene with a thickness of 10 cm is added to reduce generation of scattering neutrons; on the tapered alignment hole inner surface, the optimal thickness of boracic polyethylene is 25 cm. In this case, except reducing the scattering effect, the boracic polyethylene can reduce the leaking neutrons to enter the alignment hole; if boracic

polyethylene filtration layer is added to the alignment hole, due to serious scattering factors, it has worse result than the case where boracic polyethylene is not added. Thus, it is only necessary to add boracic polyethylene to the innermost shielding layer and alignment structure inner surface to obtain 14.1 MeV monoenergetic neutrons.

#### 4.1.2 Verification

A shielding hall in Xi'an is adopted as the background to simulate the filtration effects of different design schemes. The average neutrons and  $\gamma$  energy spectrums within the measurement zone with radius of 50 cm and interval of 1 m at a distance of 1–9 m from the source are recorded. It is assumed that the yield of neutron tube is  $5.0 \times 10^8 \text{ s}^{-1}$  (the yield of neutron tube in this paper is not less than  $5.0 \times 10^8 \text{ s}^{-1}$ ). The shielding filtration scheme is used to obtain 14.1 MeV neutrons, and the neutrons and  $\gamma$  energy spectrums are displayed in Fig. 5a, b.

Figure 6 shows that this design scheme is able to obtain 14.1 MeV neutrons with good monochromaticity. With increased radial distance, reducing of neutrons and  $\gamma$  relative fluence will be fast. The neutron energy spectral patterns at different locations are similar basically. The neutron monoenergetic peak is 14.1 MeV, while  $\gamma$  ray has some influence.

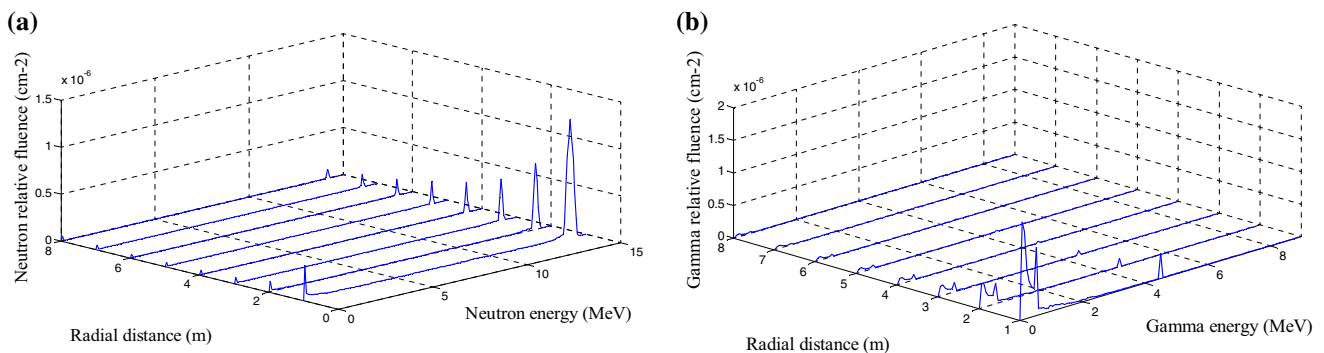


**Fig. 5** Energy spectra of neutron (a) and  $\gamma$  (b) for obtaining 14.1 MeV neutrons

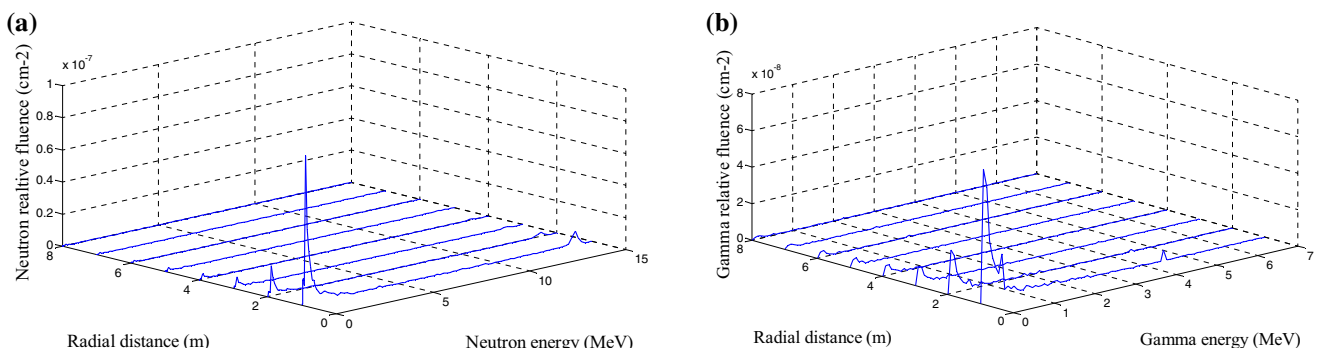


**Fig. 6** Energy spectra of neutron (a) and  $\gamma$  (b) for obtaining 0.18 MeV neutrons

## 4.2 0.18 MeV monoenergetic neutron

### 4.2.1 Design

Tungsten (W) has good shielding effect on 14 MeV fast neutron and can generate a large amount of intermediate and low-energy neutrons after being slowed down;  $B_4C$  has good shielding performance on the thermal neutrons, and when  $B_4C$  has a thickness of 0.2 cm, it can absorb all thermal neutrons. To obtain monoenergetic neutrons with energy of about 1 MeV, W material layer can be combined with 0.2 cm  $B_4C$  to filter and absorb 14 MeV fast neutrons. Through simulation of MCNP software, the result shows that with the increase in W layer thickness, high-energy 14 MeV neutrons are gradually reduced and intermediate and low-energy neutrons are gradually increasing. When the thickness of W layer is 30 cm, the ratio of intermediate and low-energy neutrons to high-energy neutrons is maximized and optimal monoenergetic neutrons can be obtained with energy peak of 0.18 MeV.

### 4.2.2 Verification

The shielding filtration scheme is used to obtain 0.18 MeV neutrons, and the neutrons and  $\gamma$  energy spectrums are displayed in Fig. 6a, b. This figure suggests that this design scheme can obtain 0.18 MeV neutrons with good monochromaticity. With increased radial distance, reducing of neutrons and relative  $\gamma$  fluence will be fast. The neutron energy spectral patterns at different locations are similar basically. The neutron monoenergetic peak is 0.18 MeV, while  $\gamma$  ray has some influence.

## 4.3 Thermal neutrons

### 4.3.1 Design

Polyethylene has good shielding performance for the intermediate and low-energy neutrons below 1 MeV, while

it has bad shielding performance for thermal neutrons. It is suggested to combine W and polyethylene as the shielding materials to obtain thermal neutrons.

The result of MCNP software simulation shows that with increased thickness of polyethylene, outgoing neutrons gradually reduce, but the neutron energy spectrums resolution gradually decreases. When the thickness of polyethylene is 4 cm and W is 30 cm, we can obtain the thermal neutron energy spectrums with best monochromaticity.

### 4.3.2 Verification

The shielding filtration scheme is used to obtain the thermal neutron structure, and the neutrons and  $\gamma$  energy spectrums are displayed in Fig. 7a, b. According to the figures, we can find that this design scheme can obtain thermal neutrons with good monochromaticity. With increased radial distance, reducing of neutrons and relative  $\gamma$  fluence will be fast. The neutron energy spectral patterns at different locations are similar basically. The neutron energy decreases below eV order, while  $\gamma$  ray has some influence.

## 4.4 Discussions about $\gamma$ ray influence

Monoenergetic outgoing points of 14.1 MeV, 0.18 MeV and thermal neutrons can be obtained by the tapered alignment filtration structure. However, some  $\gamma$  rays are produced by the filtration materials meanwhile. Monoenergetic performance will deteriorate if shielding structure used to reduce  $\gamma$  influence. To resolve the contradiction between obtaining monoenergetic neutrons and reducing  $\gamma$  influence, accurate  $\gamma$  ray monitoring equipment is suggested to apply for  $\gamma$  measurement during on-site calibration.  $\gamma$  influence can be reduced after a revision of neutron measured value. To achieve the requirement of on-site calibration, the appropriate distance between calibration position and source core is suggested due to the different neutron yield versus radial distance.

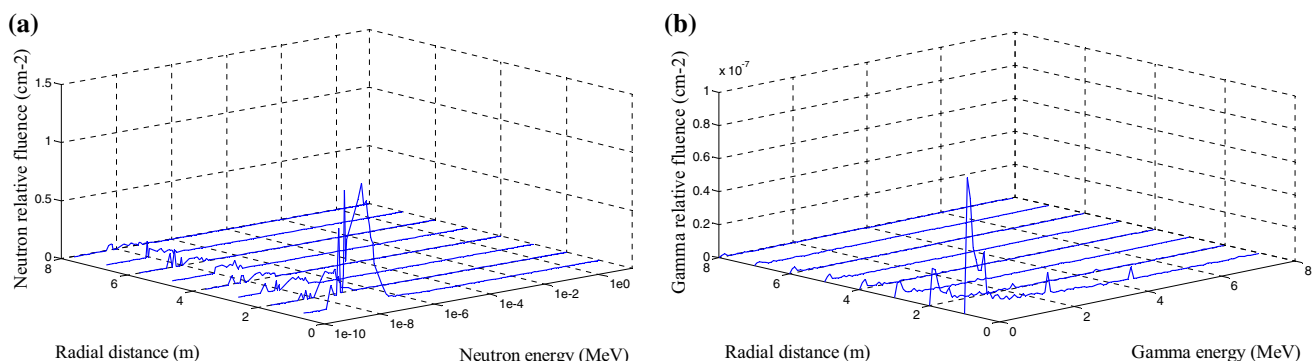


**Fig. 7** Energy spectra of neutron (a) and  $\gamma$  (b) for obtaining thermal neutrons



## 5 Conclusion

MCNP software is applied to simulate the effects of typical shielding materials and different energy neutrons. Through comparison of shielding effects by changing different material combinations, the optimal scheme can be obtained. On this base, a tapered alignment filtration structure is designed and the filtration effects of different materials are simulated to obtain the filtration schemes of monoenergetic outgoing points of 14.1 MeV, 0.18 MeV and thermal neutrons. The purpose of “multiple energies from one source” is achieved to provide reference data and technical support for on-site calibration technology research on radiation monitoring, as well as the technical reference for various neutron tubes application researches.

## References

1. J. Cub, E. Finckh, K. Gebhardt et al., The neutron detection efficiency of NE213 detectors measured by means of  $^{252}\text{Cf}$  source. *Nucl. Instrum. Methods A* **274**, 217–221 (1989)
2. M. Baba, H. Wakabayashi, M. Ishikawa, et al., Fission Spectrum Measurement of  $^{232}\text{Th}$  and  $^{238}\text{U}$  for 2 MeV Neutrons. IAEA-INDC (NDS)-220 (1989), p 149
3. Z.H. Huang, Pulse neutron logging. *Coal Geol. Expl.* **4**, 69–76 (1979). (in Chinese)
4. B.J. Wei, H.M. Zhong, *Neutron Tube & Its Application Technology* (Northeast Normal University Press, Changchun (CHN), 1997), pp. 2–3. (in Chinese)
5. Y.M. Song, H.G. Yang, J.S. Zhang, et al. Research of high yield D-T neutron tube, in Annual Report of China Institute of Atomic Energy, (2013), pp. 122–123
6. H.B. Lu, C.B. Yue, W.S. Li et al., Study of the pulsed working characteristics of the penning ion source for neutron tubes. *Nucl. Sci. Tech.* **11**, 150–154 (2000)
7. J.B. Marion, *Fast Neutron Physics* (Interscience Publishers, New York (USA), 1960), p. 1483
8. D.I. Garber. *Neutron Cross Sections*, Vol. II, 3rd edn, BNL-325 (1976)
9. M. Bastürk, J. Arztmann, W. Jerlich et al., Analysis of neutron attenuation in boron-alloyed stainless steel with neutron radiography and JEN-3 gauge. *Nucl. Mater.* **341**, 189–200 (2005)
10. Q.R. Zhang, C.L. Tang, X.Y. Chen et al., Study on preparation of composite plates with neutron shielding function. *Chem. Eng.* **23**, 76–80 (2009). (in Chinese)
11. X.Z. Cao, X.X. Xue, T. Jiang et al., Mechanical properties of UHMWPE/ $\text{Sm}_2\text{O}_3$  composite shielding material. *J. Rare Earths* **28**, 482–484 (2010). doi:[10.1016/S1002-0721\(10\)60269-4](https://doi.org/10.1016/S1002-0721(10)60269-4)
12. X.S. Xu, MCNP simulation and design of Am-Be neutron source shield. Ph.D. Thesis (Lanzhou University, 2008). (in Chinese)
13. J. Ren, X.C. Ruan, H.Q. Tang et al., Simulation of the back-ground of experimental end-stations and the collimator system of the CSNS back-streaming white neutron source. *Nucl. Tech.* **37**, 100521 (2014). doi:[10.11889/j.0253-3219.2014.hjs.37.100521](https://doi.org/10.11889/j.0253-3219.2014.hjs.37.100521). (in Chinese)
14. P.W. Lisowski, K.F. Schoenberg, The Los Alamos neutron science center. *Nucl. Instrum. Methods A* **562**, 910–914 (2006). doi:[10.1016/j.nima.2006.02.178](https://doi.org/10.1016/j.nima.2006.02.178)
15. E. Chiaveri, M. Dario, S. Andriamonje et al., *Cern n\_TOF Facility: Performance Report* (European Organization for Research, Geneva, 2003)
16. S.H. Tian, Y. Wang, X. Chen et al., Simulation and verification of neutron scattering at  $^{252}\text{Cf}$  ( $\text{D}_2\text{O}$ ) neutron laboratory. *Nucl. Tech.* **37**, 060204 (2014). doi:[10.11889/j.0253-3219.2014.hjs.37.060204](https://doi.org/10.11889/j.0253-3219.2014.hjs.37.060204). (in Chinese)
17. P. Zhang, Z.W. Zhang, Optimal design of the carbon fiber reinforcing  $\text{B}_4\text{C}/\text{Al}$  neutron absorbing materials. *Nucl. Tech.* **38**, 030605 (2015). doi:[10.11889/j.0253-3219.2015.hjs.38.030605](https://doi.org/10.11889/j.0253-3219.2015.hjs.38.030605). (in Chinese)
18. G. Vourvopoulos, P.C. Womble, Pulsed fast/thermal neutron analysis: a technique for explosives detection. *Talanta* **54**, 459–468 (2001). doi:[10.1016/S0039-9140\(00\)00544](https://doi.org/10.1016/S0039-9140(00)00544)
19. Q.L. Wei, B. Yang, Y. Wang et al., M-C simulation of slow neutron attenuation in boron-containing stainless steel. *Nucl. Tech.* **33**, 367–369 (2010). (in Chinese)
20. M. Basturk, N. Kardjilov, E. Lehmann et al., Monte Carlo simulation of neutron transmission of boron-alloyed steel. *Nucl. Sci.* **52**(1), 394–399 (2005). doi:[10.1109/TNS.2005.843638](https://doi.org/10.1109/TNS.2005.843638)